



High Voltage TAL Performance

David T. Jacobson, Robert S. Jankovsky, and Vincent K. Rawlin
Glenn Research Center, Cleveland, Ohio

David H. Manzella
University of Toledo, Toledo, Ohio

The NASA STI Program Office . . . in Profile

Since its founding, NASA has been dedicated to the advancement of aeronautics and space science. The NASA Scientific and Technical Information (STI) Program Office plays a key part in helping NASA maintain this important role.

The NASA STI Program Office is operated by Langley Research Center, the Lead Center for NASA's scientific and technical information. The NASA STI Program Office provides access to the NASA STI Database, the largest collection of aeronautical and space science STI in the world. The Program Office is also NASA's institutional mechanism for disseminating the results of its research and development activities. These results are published by NASA in the NASA STI Report Series, which includes the following report types:

- **TECHNICAL PUBLICATION.** Reports of completed research or a major significant phase of research that present the results of NASA programs and include extensive data or theoretical analysis. Includes compilations of significant scientific and technical data and information deemed to be of continuing reference value. NASA's counterpart of peer-reviewed formal professional papers but has less stringent limitations on manuscript length and extent of graphic presentations.
- **TECHNICAL MEMORANDUM.** Scientific and technical findings that are preliminary or of specialized interest, e.g., quick release reports, working papers, and bibliographies that contain minimal annotation. Does not contain extensive analysis.
- **CONTRACTOR REPORT.** Scientific and technical findings by NASA-sponsored contractors and grantees.

- **CONFERENCE PUBLICATION.** Collected papers from scientific and technical conferences, symposia, seminars, or other meetings sponsored or cosponsored by NASA.
- **SPECIAL PUBLICATION.** Scientific, technical, or historical information from NASA programs, projects, and missions, often concerned with subjects having substantial public interest.
- **TECHNICAL TRANSLATION.** English-language translations of foreign scientific and technical material pertinent to NASA's mission.

Specialized services that complement the STI Program Office's diverse offerings include creating custom thesauri, building customized data bases, organizing and publishing research results . . . even providing videos.

For more information about the NASA STI Program Office, see the following:

- Access the NASA STI Program Home Page at <http://www.sti.nasa.gov>
- E-mail your question via the Internet to help@sti.nasa.gov
- Fax your question to the NASA Access Help Desk at 301-621-0134
- Telephone the NASA Access Help Desk at 301-621-0390
- Write to:
NASA Access Help Desk
NASA Center for Aerospace Information
7121 Standard Drive
Hanover, MD 21076



High Voltage TAL Performance

David T. Jacobson, Robert S. Jankovsky, and Vincent K. Rawlin
Glenn Research Center, Cleveland, Ohio

David H. Manzella
University of Toledo, Toledo, Ohio

Prepared for the
37th Joint Propulsion Conference and Exhibit
cosponsored by the AIAA, SAE, AIChE, and ASME
Salt Lake City, Utah, July 8–11, 2001

National Aeronautics and
Space Administration

Glenn Research Center

Available from

NASA Center for Aerospace Information
7121 Standard Drive
Hanover, MD 21076

National Technical Information Service
5285 Port Royal Road
Springfield, VA 22100

Available electronically at <http://gltrs.grc.nasa.gov/GLTRS>

High Voltage TAL Performance

David T. Jacobson, Robert S. Jankovsky, and Vincent K. Rawlin
National Aeronautics and Space Administration
Glenn Research Center
Cleveland, Ohio 44135

David H. Manzella
University of Toledo
Toledo, Ohio 43606

Abstract

The performance of a two-stage, anode layer Hall thruster was evaluated. Experiments were conducted in single and two-stage configurations. In single-stage configuration, the thruster was operated with discharge voltages ranging from 300 to 1700 Volts. Discharge specific impulses ranged from 1630 to 4140 seconds. Thruster investigations were conducted with input power ranging from 1 kW to 8.7 kW, corresponding to power throttling of nearly 9:1. An extensive two-stage performance map was generated. Data taken with total voltage (sum of discharge and accelerating voltage) constant revealed a decrease in thruster efficiency as the discharge voltage was increased. Anode specific impulse values were comparable in the single and two-stage configurations showing no strong advantage for two-stage operation.

Introduction

It is well known that the use of electric propulsion can reduce the on-board propulsion system mass, thereby decreasing spacecraft launch mass or increasing payload capability. Typically, different electric propulsion devices satisfy different mission requirements based on their inherent characteristics. For example, gridded ion thrusters better satisfy interplanetary mission requirements, where mission benefit is derived through high specific impulse operation.¹ Conversely, the relatively high thrust density of Hall thrusters is well suited to lower specific impulse maneuvers such as orbit raising where reasonable trip times are required.² Even greater mission benefits may be realized by increasing the upper limit of specific impulse attainable by current Hall thrusters, which has traditionally been limited to 1500-1700 seconds.¹

In an attempt to extend the operational envelope of state-of-the-art (SOA) Hall thrusters, NASA

Glenn Research Center (GRC) awarded two contracts to develop a Hall thruster with the following characteristics: power=2.3 kW, thrust=100 mN, Isp=3200 seconds (s), lifetime=8000 hours. A magnetic layer thruster was developed under the contract with Atlantic Research Corporation and delivered to NASA for evaluation. The results of this investigation are presented in a paper authored by Manzella.³ Another Hall thruster of the anode layer type (TAL) was developed under contract NAS3-99171, with Boeing Rocketdyne.⁴ The thruster was designed and fabricated by Central Research Institute of Machine Building (TsNIMASH), Boeing's subcontractor. This thruster, designated D-80, was evaluated at NASA GRC.

The objective of this work was to investigate the operating characteristics of the D-80 in a high discharge voltage regime compared to SOA Hall thruster discharge voltages (300-500 Volts). The performance of the device was measured in both

the traditional single-stage, and two-stage configurations. The results of these investigations are presented herein.

Apparatus

The thruster under consideration is a laboratory model TAL designated D-80. The model designation refers to the average diameter of the discharge chamber in millimeters. The thruster employs a segmented anode consisting of two electrodes. This geometry enables operation in single and two-stage configurations. Two-stage thruster operation allows different electric potentials to be applied between the two electrodes, thereby allowing modification of the electric field distribution. The discharge voltage is applied between the first and second stage anode electrodes and the accelerating voltage is applied between the cathode and second stage anode. In this configuration, ionization is desired in the first stage region, followed by acceleration of the ions in the second stage⁵. For single-stage operation, the first and second stage electrodes are electrically connected, allowing a single potential difference to be applied between anode and cathode. The D-80 Hall thruster is described in detail elsewhere.⁶ A photograph and mechanical schematic drawing of the D-80 thruster are provided as Figures 1 and 2, respectively.

The hollow cathode used was manufactured by Semicon and was similar in design to the NASA plasma contactor design. The cathode was a laboratory model unit operated at a nominal flow rate of 0.4 mg/s throughout testing. The cathode was mounted at a 45° angle with respect to the thruster axis as shown in Figure 1. The cathode orifice was located 0.03 m downstream of the thruster exit plane and 0.025 m radially from the outer pole piece.⁵

Thrust was measured continuously on a NASA GRC designed inverted pendulum thrust stand. The thrust stand used has been described in detail elsewhere.^{7,8} The stand employed a closed

loop inclination control circuit, which utilized a piezoelectric element to minimize thermal drift. Calibration was performed in-situ using three 0.01 kg masses applied along the thrust vector over a pulley.

The power system utilized commercially available power supplies. Separate supplies were used to power the inner and outer magnets, cathode heater, and keeper. The discharge circuit consisted of two power supplies enabling thruster operation in single or two-stage configurations. For single-stage operation, a switch was used to short the discharge power supply, electrically connecting the two electrodes together. In the two-stage configuration, the discharge supply was located between the first and second stage anode electrodes, and the accelerating supply was located between cathode and second stage anode. Simple output filters, consisting of 10 and 100 μ F capacitors were used. The capacitors were located across the discharge and accelerating electrodes, and the accelerating electrode and cathode, respectively. Two 70 V Zener diodes were placed back-to-back from cathode common to ground to clamp the cathode floating potential. The cathode floating potential was not more than 13 volts (V) negative with respect to ground during testing. A schematic drawing of the electrical configuration is provided in Figure 3.

All testing was performed in NASA Glenn's Vacuum Facility 6 (VF 6). VF 6 is an oil free facility, which employs 12 cryopumps, each with a liquid nitrogen shroud. At the highest xenon mass flow rate of 8 mg/s, the indicated facility pressure was 2.0×10^{-4} Pa as measured on ion gauges calibrated for air. The main chamber has a 7.6 m diameter and length of 22 m. The test hardware was located in a 3 m diameter belljar connected to the main chamber. The belljar has isolation capability allowing the access to the hardware without venting the main chamber to atmosphere. A photograph of the test apparatus is provided in Figure 4.

Results and Discussion

The D-80 thruster was operated in both single and two-stage configurations over a wide range of mass flow rates and discharge voltages. The range was selected to define the possible operating envelope and allow for a broad comparison of single and two-stage data. In the single-stage configuration, data were initially collected for mass flow rates between 4 and 8 mg/s and discharge voltages between 300 and 900 V. This range was subsequently extended to include discharge voltages up to 1700 V. Thruster operation was investigated in the two-stage configuration over discharge voltages from 300-1000 V and a fixed discharge voltage of 100 V for a range of mass flow rates from 4-8 mg/s. First, the single-stage data will be presented, followed by the two-stage data, and finally the results of the two configurations will be compared.

Single-stage Operation

The D-80 single-stage operational envelope is depicted in Figure 5. All single-stage data, ranging from 300 V to 1600 V in 100 V increments are presented. Measured thrust ranged from a minimum value of 64 mN at 300 V and 3.3 A, to a maximum of 240 mN at 1700 V and 5.1 A. Thruster investigations were conducted with input power ranging from 1 kW to 8.7 kW, corresponding to power throttling of nearly 9:1. Temperature measurements indicated that operation above 4 kW potentially exceeded the steady-state thermal capability of the thruster. These data are provided in Table 1.

Thruster operation was stable over this power range. The exception to this was at voltages above 1000 V where periodic, short duration, occurrences of current limited operation were experienced. These events typically only occurred during transient periods when the discharge voltage or anode mass flow rate was being adjusted. Slow and deliberate adjustment mitigated this anomalous behavior.

The D-80 single-stage, anode specific impulse is plotted versus discharge voltage for anode mass flow rates ranging from 3 to 8 mg/s in Figure 6. Anode specific impulse is defined as the specific impulse calculated excluding the cathode flow. The discontinuities in the 4, 5, 6 mg/s cases were attributed to small differences in anode mass flow rate between data taken on different days, and incomplete optimization of the inner and outer magnet currents for every point. Initial test data were taken at mass flow rates between 4-8 mg/s and discharge voltages from 300-900 V. The stable operation of the thruster at these elevated voltages suggested that higher discharge voltages were obtainable; as a result, data were subsequently obtained at discharge voltages between 900 and 1700 V.

For these data the anode specific impulse ranged from 1630 s at 300 V and 3.3 A to a maximum of 4140 s at 1700 V and 5.1 A. In all cases, the anode specific impulse increased nearly monotonically with increasing flow rate and voltage. The anode specific impulse increased less rapidly with increasing discharge voltages for voltages above 700 Volts. A curve fit to the specific impulse data was nearly proportional to square root of the discharge voltage as expected. The 3 mg/s mass flow rate data does not exhibit this trend. At voltages above 1100 V that anode specific impulse decreased.

Anode efficiency is plotted versus discharge voltage in Figure 7 for the same single-stage data. For a given anode mass flow rate the maximum efficiency corresponded to discharge voltages ranging from 500-800 V. After this point, the efficiency decreased with increasing voltage. The anode efficiency data suggested that a loss mechanism was enhanced at these higher voltages. While sufficient data does not exist to definitively identify this mechanism, similar trends have been observed with the SPT device operated at elevated voltages³.

These data also suggest the thruster was oversized for optimum performance at 2.3 kW. For example, at 2.3 kW with a discharge voltage of 700 V and a discharge current of 3.2 A the thrust was 97 mN. This corresponds to an anode specific impulse of 2480 s and an anode efficiency of 53%, which approaches the desired target thrust of 100 mN albeit at 700 s below the target of 3200 s. In contrast, at 5.2 kW with a discharge voltage of 800 Volts and a discharge current of 6.5 Amperes the thrust was 224 mN. The anode specific impulse and efficiency at this point are 3320 s and 71%, respectively. In general, all these data reflected this trend, i.e. the specific impulse and efficiency increased for a given discharge voltage with increasing anode mass flow rate. It is however anticipated that operation at these high power densities would have an adverse effect on the thermal operating regime of the thruster and thruster life.

Two-Stage Operation

D-80 thruster operation in the two-stage configuration was also investigated extensively. Tests were conducted over a range of mass flow rates from 4-8 mg/s with discharge voltages from 0 to 200 V, and a constant accelerating voltage of 600 V in an attempt to identify an optimal discharge voltage at which to evaluate two-stage performance. The results of these tests were inconclusive, but a discharge voltage of 100 V was selected for further testing based on previously published test results.⁹ Performance was then evaluated for anode mass flow rates between 4 and 8 mg/s, a constant discharge voltage of 100 V, and accelerating voltages between 300 and 1000 V. For these data the measured thrust ranged from 74 mN to 278 mN and the anode specific impulse ranged from 1890 s to 3610 s. In general, the highest efficiency data points corresponded to the highest mass flow rate and accelerating voltages as was seen during single-stage operation. These data are presented in Table 2.

Due to the inconclusive result of the discharge voltage variation, a second approach for investigating two-stage operation was implemented. For these tests the thruster was operated with a constant total voltage, that is the sum of the discharge voltage and the accelerating voltage was constant. In the case of a constant total voltage of 800 V, for example, the thruster would be operated with discharge voltage of 100 V and accelerating voltage of 700 V. Subsequent points would then be taken at discharge and accelerating voltages of 125 and 675 V respectively. A single-stage point was also included in each constant voltage data series. A comprehensive tabulation of these data is presented in Table 3.

Data with constant total voltage of 800V are presented in Figure 8. Anode efficiency and thrust are plotted versus discharge voltage for anode mass flow rates of 6 and 7 mg/s. In both cases, the peak anode efficiency was measured during single-stage operation, or where discharge voltage was zero. As the discharge voltage was increased, and the accelerating voltage decreased, the efficiency decreased. The measured thrust over these data sets remained constant. However, as the discharge voltage was increased, the total power increased. This caused the drop in efficiency.

The concept that the ionization and acceleration regions can be separated in the first and second stage of the thruster during two-stage operation seems to be contradicted by the constant measured thrust. By maintaining as much as 200 V between the first and second stage electrodes there is 200 V less for acceleration in the external anode layer. Because the thrust was unchanged the thrust producing ions were necessarily created upstream of the first stage to second stage gap and were subsequently accelerated through this region. This further suggests that for the conditions tested the ionization efficiency was extremely good. This conclusion is also supported by the fact that

thrust was constant for various combinations of discharge and accelerating voltage. That is, the ions seem to be accelerated through the same total voltage regardless of how it was distributed within the channel. Interestingly, two-stage operation with zero voltage between the first and second stages operated with zero discharge current. This suggests that even during single-stage operation very little of the discharge current is being collected in the upstream part of the anode. Additional experiments would need to be conducted to definitively prove each of these conclusions.

Additional tests with different anode mass flow rates and different total voltages are presented in Figure 9. Five cases are for constant total voltage of 800 V and anode mass flow rates from 3-7 mg/s and two cases are for an anode mass flow rate of 6 mg/s and constant total voltages of 600 and 1000 V. With the exception of the constant total voltage of 800V, 4 mg/s case, the trends exhibited by the 6 and 7 mg/s and 800 V constant total voltage were repeated. That is the anode efficiency decreased with increasing discharge voltage. In the 4 mg/s case, the efficiency begins to decrease with increasing discharge voltage up to 25.0 V, then begins to increase to a maximum at 100-125 V. This suggests that some performance benefit may be realized in the two-stage configuration at low anode mass flow rates. Specifically, this case represented the lowest flow rate, and as a result, lowest channel density case considered. Under these conditions the ionization efficiency may have in fact been enhanced through the use of the first stage anode as was originally expected.

Single and Two-Stage Comparison

In order to allow for a direct comparison of single versus two-stage operation, the data presented in Figure 10 were taken at various constant input powers. In this figure, anode specific impulse is plotted versus thrust for power levels ranging from 2-7 kW. In the 6 and

7 kW cases, only two-stage data were available. In the other cases, there is no appreciable difference between the single and two-stage points at a given power level and the points lie approximately on the same line. This behavior is indicative of similar performance characteristics in the two separate operating configurations.

Lastly, anode specific impulse is compared at equivalent voltages for mass flow rate cases of 5, 6 and 7 mg/s. These data are depicted in Figure 11. For the two-stage points, the voltage used on the abscissa is the sum of the accelerating and discharge voltages. The data are very similar at all points regardless of flow rate or voltage. The two-stage configuration anode specific impulse exceeds that of the single-stage configuration for all but two data points. The difference in magnitude between the specific impulse values is between 1 and 3% in all cases. This difference is not statistically significant, and seems to indicate that this thruster performs similarly in the single and two-stage configurations.

Conclusions

The D-80 Hall thruster was operated in single and two-stage configurations. In single-stage configuration, specific impulse in excess of 4000 s and efficiency over 70% was demonstrated. Stable operation was achieved at voltages over 1600 V. Thruster investigations were conducted with input power ranging from 1 kW to 8.7 kW, corresponding to power throttling of nearly 9:1.

A two-stage performance map was generated using a discharge voltage of 100 V. Two-stage thruster operation was conducted at power levels ranging from 1.3 to 8.2 kW. Demonstrated specific impulse ranged from 1900 to 3600 s over this range. Additional testing was conducted, holding the sum of the discharge and accelerating voltage constant. It was apparent that the single-stage performance was equivalent to the performance in the two-stage configuration with zero discharge voltage. Any discharge voltage increase had a negative effect

on efficiency, as the power consumed in the first stage created inefficiency in the thruster operation.

The original target parameters were a power level of 2.3 kW, thrust of 100 mN, and specific impulse of 3200 s. While these parameters were not demonstrated at a single point, the thruster operated in a stable fashion and performed well over an extremely wide envelope. Maximum performance was demonstrated at a discharge voltage of 800 V and discharge current of 6.5 A. The anode specific impulse, thrust and efficiency were 3320 s, 224 mN and 71 %, respectively.

A cursory investigation revealed that the steady state thermal limit of the thruster may be 4 kW. While a portion of the operating points were above this power level, improvements in the thruster's design could potentially be employed to circumvent this issue.

References

1. Oleson, S. R., "Mission Advantages of Constant Power, Variable Isp Electrostatic Thrusters," AIAA-2000-3413, July 2000.
2. Oleson, S.R., Sankovic, J.M., "Advanced Hall Electric Propulsion for Future In-Space Transportation," NASA TM-2001-210676.
3. Manzella, D.H., *et al.*, "High Voltage SPT Operation," AIAA-2001-3774, July 2001.
4. Yuen, J.L., Tverdokhlebov, S.O., Semenkin, A.V., "Hall Thruster Development-Anode Layer Thruster D-80," NAS3-99171 Final Report, April 2000.
5. Rocketdyne/TsNIIMASH Team, "Anode Layer Thruster D-80 Operation Manual," Hall Thruster Development Contract No. NAS3-99171, January 2000.
6. Butler, G.W., *et al.*, "Multi-Mode, High Specific Impulse Hall Thruster Technology," AIAA-2000-3254, July 2000.
7. Haag, T.W., Manzella, D.M., "RHETT/EPDM Performance Characterization," IEPC-97-107, August 1997.
8. Jacobson, D.T., Jankovsky, R.S., "Test Results of a 200 W Class Hall Thruster," NASA TM-1999-209449.
9. Tverdokhlebov, S., "Study of Double-Stage Anode Layer Thruster Using Inert Gases," IEPC-93-232, September 1993.

Table 1: D-80 Single Stage Data

Discharge		Discharge Power, W	Inner Magnet		Outer Magnet		Total Power, W	Flow Rates, mg/s		Cat float Voltage, V	Thrust mN	Isp sec	Isp* sec	Eff	Eff*
Volts	Amps		Volts	Amps	Volts	Amps		Cath	Anode						
809.7	2.3	1838	2.1	0.71	1.7	0.23	1840	0.4	3.0	-8.8	72	2153	2440	0.41	0.47
900.1	2.3	2043	1.5	0.49	2.4	0.31	2045	0.4	3.0	-9.7	79	2370	2687	0.45	0.51
998.8	2.2	2187	1.6	0.52	3.2	0.41	2190	0.4	3.0	-10.1	81	2423	2747	0.44	0.50
1100.4	2.3	2487	1.6	0.49	2.2	0.27	2488	0.4	3.0	-9.3	84	2503	2838	0.41	0.47
1200.0	2.1	2532	1.4	0.44	3.9	0.47	2534	0.4	3.0	-9.9	81	2431	2756	0.38	0.43
1299.3	2.1	2716	1.6	0.47	3.7	0.43	2718	0.4	3.0	-9.8	82	2464	2794	0.37	0.41
1400.7	2.1	2899	1.7	0.52	3.7	0.43	2902	0.4	3.0	-8.9	78	2345	2659	0.31	0.35
300.0	3.3	1002	2.8	0.70	3.1	0.38	1005	0.4	4.0	-10.6	64	1483	1633	0.46	0.51
400.0	3.3	1328	2.8	0.70	3.1	0.38	1331	0.4	4.0	-10.8	74	1725	1899	0.47	0.52
500.0	3.3	1630	2.8	0.70	3.1	0.38	1633	0.4	4.0	-10.9	83	1933	2128	0.48	0.53
600.0	3.2	1944	2.8	0.70	3.2	0.38	1947	0.4	4.0	-10.3	90	2092	2304	0.47	0.52
700.0	3.2	2240	2.8	0.70	3.2	0.38	2243	0.4	4.0	-11.5	97	2254	2481	0.48	0.53
800.0	3.2	2536	2.8	0.70	3.2	0.38	2539	0.4	4.0	-11.4	102	2384	2624	0.47	0.52
900.0	3.1	2826	2.8	0.70	3.3	0.38	2829	0.4	4.0	-11.4	107	2497	2748	0.46	0.51
300.0	3.2	966	2.9	0.70	3.3	0.38	969	0.4	4.0	-11.5	62	1449	1596	0.46	0.50
799.7	3.3	2607	2.6	0.73	4.1	0.44	2611	0.4	4.0	-9.7	107	2495	2745	0.50	0.56
900.4	3.2	2890	2.8	0.74	4.9	0.50	2895	0.4	4.0	-9.9	113	2628	2892	0.50	0.56
1000.5	3.1	3132	3.1	0.81	5.3	0.54	3137	0.4	4.0	-10.2	117	2727	3001	0.50	0.55
1100.0	3.1	3454	3.0	0.76	4.8	0.48	3459	0.4	4.0	-9.7	122	2840	3125	0.49	0.54
1200.0	3.2	3804	2.8	0.68	4.7	0.46	3808	0.4	4.0	-9.5	127	2948	3245	0.48	0.53
1300.0	3.2	4108	3.0	0.71	5.3	0.50	4113	0.4	4.0	-9.3	129	3000	3301	0.46	0.51
1400.4	3.1	4369	2.8	0.65	5.2	0.48	4374	0.4	4.0	-9.5	133	3081	3391	0.46	0.51
1499.2	3.1	4633	3.0	0.66	5.4	0.49	4637	0.4	4.0	-10.8	134	3120	3434	0.44	0.49
1600.8	3.1	4898	3.0	0.66	5.5	0.49	4903	0.4	4.0	-10.1	137	3192	3513	0.44	0.48
300.6	4.4	1332	3.6	1.23	4.6	0.72	1339	0.4	4.9	-9.8	85	1625	1756	0.51	0.55
400.4	4.3	1730	3.6	1.22	4.0	0.61	1737	0.4	4.9	-10.1	98	1873	2025	0.52	0.56
500.6	4.3	2128	3.5	1.19	4.5	0.68	2135	0.4	4.9	-10.7	110	2092	2261	0.53	0.57
599.9	4.2	2490	3.0	0.98	3.4	0.51	2494	0.4	4.9	-9.9	120	2286	2471	0.54	0.58
699.9	4.1	2877	2.6	0.87	3.6	0.52	2881	0.4	4.9	-9.7	127	2428	2625	0.53	0.57
799.9	4.1	3256	2.4	0.78	3.3	0.47	3259	0.4	4.9	-9.5	135	2579	2788	0.52	0.57
900.7	4.0	3603	2.6	0.83	3.9	0.54	3607	0.4	4.9	-9.6	140	2670	2887	0.51	0.55
800.1	4.3	3400	4.5	0.94	5.6	0.49	3407	0.4	4.9	-10.7	140	2670	2887	0.54	0.58
901.4	4.2	3804	4.2	0.86	6.0	0.51	3811	0.4	4.9	-10.5	148	2824	3053	0.54	0.58
1000.0	4.2	4180	4.3	0.86	6.0	0.51	4187	0.4	4.9	-10.4	155	2949	3188	0.53	0.58
1097.9	4.1	4545	4.1	0.81	7.1	0.60	4553	0.4	4.9	-10.0	161	3073	3323	0.53	0.58
1200.3	4.2	4981	4.0	0.77	7.0	0.59	4988	0.4	4.9	-10.5	168	3198	3457	0.53	0.57
1301.6	4.1	5311	4.4	0.82	7.1	0.59	5318	0.4	4.9	-10.7	173	3297	3565	0.53	0.57
1401.3	4.1	5675	4.5	0.82	7.1	0.58	5683	0.4	4.9	-10.6	178	3400	3675	0.52	0.57
1500.4	4.0	6047	4.2	0.74	7.9	0.64	6055	0.4	4.9	-11.0	183	3487	3770	0.52	0.56
1600.0	4.0	6464	3.8	0.67	7.9	0.64	6472	0.4	4.9	-10.6	186	3543	3831	0.50	0.54
300.2	5.4	1633	4.1	1.35	2.5	0.37	1639	0.4	5.9	-10.9	105	1692	1807	0.53	0.57
400.0	5.4	2140	4.1	1.35	2.5	0.37	2146	0.4	5.9	-11.5	121	1960	2092	0.54	0.58
500.0	5.2	2620	4.1	1.35	2.5	0.37	2626	0.4	5.9	-11.5	135	2185	2333	0.55	0.59
601.9	5.2	3124	3.4	1.10	3.8	0.56	3130	0.4	5.9	-12.0	150	2429	2593	0.57	0.61
700.1	5.2	3606	3.4	1.08	3.9	0.57	3611	0.4	5.9	-11.5	162	2609	2786	0.57	0.61
800.9	5.1	4077	3.4	1.07	4.0	0.56	4082	0.4	5.9	-10.4	169	2726	2910	0.55	0.59
900.4	5.1	4565	3.2	0.95	5.4	0.66	4572	0.4	5.9	-10.3	177	2849	3042	0.54	0.58
800.3	5.4	4322	5.7	0.98	9.0	0.71	4334	0.4	5.9	-10.9	181	2932	3130	0.60	0.64
900.3	5.3	4790	6.5	1.08	8.8	0.69	4803	0.4	5.9	-10.7	191	3082	3291	0.60	0.64
1006.5	5.3	5334	5.6	0.92	7.3	0.57	5344	0.4	5.9	-10.4	199	3216	3434	0.59	0.63
1100.8	5.3	5779	5.6	0.91	7.4	0.57	5789	0.4	5.9	-10.3	206	3335	3562	0.58	0.62
1201.1	5.2	6282	5.7	0.91	6.8	0.53	6291	0.4	5.9	-10.0	212	3429	3661	0.57	0.61
1300.3	5.2	6723	6.0	0.96	6.7	0.52	6732	0.4	5.9	-9.9	218	3519	3758	0.56	0.60
1400.4	5.2	7282	5.6	0.88	6.7	0.52	7291	0.4	5.9	-9.8	224	3616	3861	0.54	0.58
1497.4	5.2	7801	5.1	0.78	7.6	0.58	7810	0.4	5.9	-10.3	229	3700	3952	0.53	0.57
1600.7	5.2	8292	5.1	0.78	7.7	0.58	8300	0.4	5.9	-10.8	235	3799	4057	0.53	0.56
1699.0	5.1	8733	5.2	0.78	7.7	0.58	8741	0.4	5.9	-10.8	240	3879	4142	0.52	0.56
301.6	6.6	1985	5.7	1.61	4.5	0.53	1996	0.4	6.9	-10.5	126	1759	1862	0.54	0.58
400.0	6.4	2556	5.8	1.61	4.6	0.53	2568	0.4	6.9	-11.8	145	2034	2152	0.56	0.60
500.0	6.3	3135	5.9	1.61	4.6	0.53	3147	0.4	6.9	-11.9	163	2287	2420	0.58	0.62
601.5	6.2	3705	5.5	1.43	5.1	0.57	3716	0.4	6.9	-11.6	179	2509	2655	0.59	0.63
701.4	6.1	4265	5.4	1.38	4.5	0.50	4274	0.4	6.9	-10.9	192	2682	2838	0.59	0.63
800.1	6.3	5057	5.5	1.38	4.6	0.50	5066	0.4	6.9	-10.6	213	2975	3148	0.61	0.65
300.7	7.8	2351	5.1	1.24	4.8	0.51	2360	0.4	7.9	-9.6	148	1831	1925	0.56	0.60
400.2	7.7	3078	5.2	1.24	4.9	0.50	3086	0.4	7.9	-10.1	173	2141	2251	0.59	0.62
499.5	7.5	3721	6.1	1.41	4.9	0.50	3732	0.4	7.9	-11.1	192	2372	2493	0.60	0.63
600.2	7.3	4387	6.2	1.41	5.0	0.50	4399	0.4	7.9	-11.0	210	2594	2726	0.61	0.64
700.6	7.2	5009	7.2	1.59	5.4	0.53	5024	0.4	7.9	-10.8	225	2780	2922	0.61	0.64

* Indicates values calculated with discharge power only and without cathode flow.

Table 2: D-80 Two-Stage Constant Discharge Voltage Data

Discharge		Accelerator		Inner Magnet		Outer Magnet		Total Power, W	Flow Rates, mg/s		Cat to Grd. V	Thrust mN	Isp sec	Isp* sec	Eff	Eff*
Volts	Amps	Volts	Amps	Volts	Amps	Volts	Amps		Cathode	Anode						
100.7	3.7	300.0	3.2	3.1	0.71	4.9	0.50	1343	0.4	4.0	-7.8	74	1717	1890	0.46	0.51
101.0	3.6	400.0	3.2	3.1	0.71	5.0	0.50	1658	0.4	4.0	-7.6	83	1944	2140	0.48	0.53
100.6	3.3	500.0	3.0	3.2	0.71	6.5	0.65	1851	0.4	4.0	-7.6	90	2098	2310	0.50	0.55
100.9	3.3	600.8	3.0	3.3	0.71	6.6	0.65	2161	0.4	4.0	-10.1	96	2241	2467	0.49	0.54
101.2	3.3	700.8	3.0	3.3	0.71	6.6	0.65	2431	0.4	4.0	-10.3	102	2367	2605	0.49	0.54
100.0	3.2	800.6	2.9	3.4	0.71	6.7	0.65	2679	0.4	4.0	-10.3	107	2483	2733	0.48	0.53
100.6	3.2	900.4	2.9	3.4	0.71	5.9	0.58	2974	0.4	4.0	-9.9	113	2630	2896	0.49	0.54
100.9	3.2	1000.7	2.9	3.5	0.71	5.2	0.50	3267	0.4	4.0	-9.6	118	2739	3015	0.48	0.53
99.5	4.8	300.0	4.2	3.9	0.77	5.4	0.50	1756	0.4	4.9	-9.4	98	1874	2026	0.51	0.56
100.0	4.7	400.0	4.2	4.0	0.77	5.4	0.50	2145	0.4	4.9	-9.5	111	2124	2296	0.54	0.59
100.3	4.7	500.0	4.2	4.0	0.77	5.4	0.50	2547	0.4	4.9	-9.5	121	2310	2497	0.54	0.58
100.5	4.1	600.0	4.1	4.0	0.77	5.0	0.46	2873	0.4	4.9	-9.2	128	2449	2648	0.54	0.58
100.7	4.5	700.0	4.1	4.1	0.77	5.0	0.46	3300	0.4	4.9	-9.2	136	2584	2794	0.52	0.56
100.9	4.4	800.2	4.0	4.1	0.77	5.0	0.46	3659	0.4	4.9	-9.2	141	2696	2915	0.51	0.55
101.3	4.4	900.2	4.0	4.1	0.77	4.6	0.43	4040	0.4	4.9	-9.0	146	2793	3020	0.50	0.54
101.5	4.4	1001.0	4.0	4.1	0.77	4.6	0.43	4413	0.4	4.9	-9.0	152	2896	3131	0.49	0.53
100.2	6.3	300.2	5.5	4.1	0.74	5.1	0.46	2273	0.4	5.9	-8.6	124	2009	2145	0.54	0.58
100.3	6.0	400.0	5.4	4.1	0.74	5.1	0.46	2749	0.4	5.9	-8.9	139	2250	2403	0.56	0.60
100.5	6.0	500.2	5.4	4.1	0.74	5.1	0.46	3290	0.4	5.9	-9.1	151	2433	2598	0.55	0.58
100.8	5.9	600.1	5.2	4.7	0.84	5.0	0.45	3742	0.4	5.9	-8.9	161	2592	2768	0.55	0.58
101.0	5.8	700.1	5.2	4.8	0.84	5.1	0.45	4215	0.4	5.9	-8.8	170	2738	2924	0.54	0.58
101.0	5.8	800.0	5.1	4.8	0.84	5.1	0.45	4675	0.4	5.9	-8.8	178	2874	3069	0.54	0.57
101.0	5.7	900.0	5.1	4.9	0.84	5.1	0.45	5152	0.4	5.9	-8.8	185	2993	3196	0.53	0.57
101.6	5.4	1000.0	4.9	6.0	1.00	5.7	0.48	5440	0.4	5.9	-8.7	190	3070	3278	0.53	0.56
100.4	7.7	300.1	6.6	6.1	1.00	5.7	0.48	2771	0.4	6.9	-9.2	149	2079	2200	0.55	0.58
100.6	7.5	400.0	6.5	6.2	1.00	5.8	0.48	3378	0.4	6.9	-9.2	167	2343	2479	0.57	0.60
100.7	7.4	500.0	6.4	6.2	1.00	5.8	0.48	3965	0.4	6.9	-9.2	182	2547	2696	0.57	0.61
100.9	7.2	600.5	6.3	6.3	1.00	5.8	0.48	4540	0.4	6.9	-9.1	195	2725	2883	0.57	0.61
101.0	7.1	700.7	6.3	6.4	1.00	5.1	0.41	5107	0.4	6.9	-9.0	205	2869	3036	0.57	0.60
101.4	7.0	800.0	6.2	6.4	1.00	4.2	0.34	5703	0.4	6.9	-9.0	214	2995	3170	0.55	0.58
101.6	7.0	900.0	6.2	6.4	0.99	4.2	0.34	6295	0.4	6.9	-9.0	224	3127	3310	0.54	0.58
101.7	6.9	1000.0	6.2	6.5	0.99	4.2	0.34	6883	0.4	6.9	-8.9	232	3241	3429	0.54	0.57
66.5	9.1	299.8	7.8	6.9	1.02	10.3	0.81	2960	0.4	7.9	-9.4	165	2033	2137	0.56	0.59
71.2	9.0	400.0	7.7	7.0	1.03	10.4	0.81	3734	0.4	7.9	-9.8	189	2336	2455	0.58	0.61
78.2	8.9	500.2	7.6	7.0	1.03	10.4	0.81	4520	0.4	7.9	-9.8	211	2603	2736	0.60	0.63
100.0	8.7	600.4	7.6	6.6	0.96	7.6	0.59	5465	0.4	7.9	-9.3	231	2858	3004	0.59	0.63
100.3	8.6	700.0	7.5	6.6	0.96	7.6	0.59	6141	0.4	7.9	-9.2	245	3029	3183	0.59	0.62
100.6	8.5	800.0	7.4	6.7	0.96	7.6	0.59	6815	0.4	7.9	-9.1	258	3184	3347	0.59	0.62
101.0	8.4	900.0	7.4	6.7	0.96	7.6	0.59	7499	0.4	7.9	-9.1	269	3322	3491	0.58	0.62
101.2	8.3	1000.0	7.3	6.7	0.96	7.6	0.59	8168	0.4	7.9	-9.0	278	3430	3606	0.57	0.60

*Indicates values calculated with discharge power only and without cathode flow.

Table 3: D-80 Two-Stage Constant Total Voltage Data

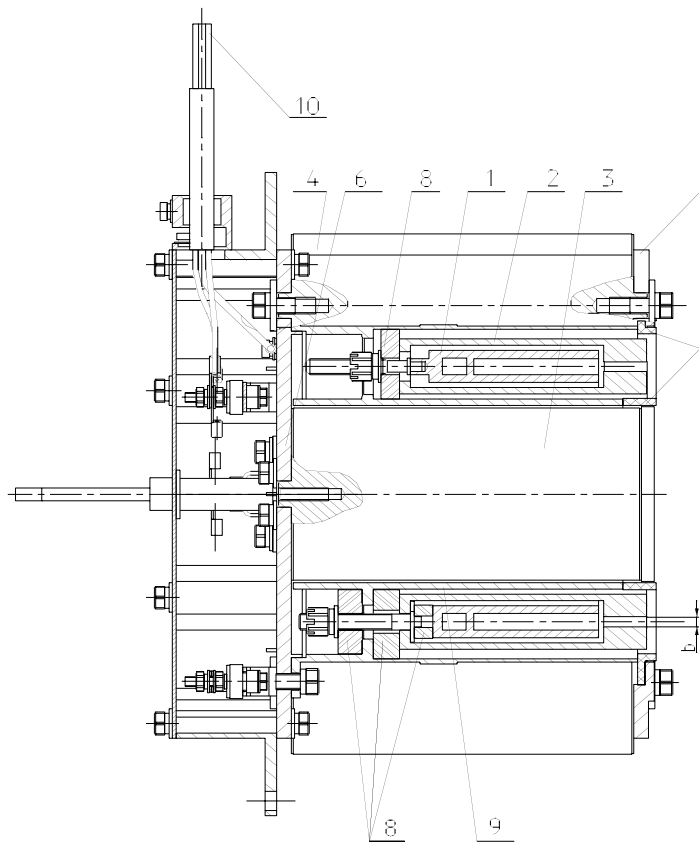
Discharge		Accelerator		Total V	Inner Mag.		Outer Mag.		Total	Flow Rates, mg/s		Cathode	Thrust	Isp	Isp*	Eff	Eff*
Volts	Amps	Volts	Amps	Volts	Volts	Amps	Volts	Amps	Power, W	Cath.	Anode	to Grd. (V)	mN	sec	sec		
**		801.7	2.4	802.0	1.6	0.57	2.5	0.40	1910	0.4	3.0	-9.6	78	2348	2661	0.47	0.54
5.2	1.5	795.6	2.2	800.8	3.0	0.53	4.4	0.40	1778	0.4	3.0	-10.8	76	2275	2579	0.48	0.54
9.9	2.0	790.5	2.2	800.4	2.9	0.52	4.5	0.40	1786	0.4	3.0	-10.8	76	2276	2580	0.47	0.54
25.6	2.3	775.9	2.2	801.5	3.3	0.59	4.5	0.40	1776	0.4	3.0	-11.2	77	2310	2619	0.49	0.56
50.1	2.4	750.5	2.3	800.6	2.8	0.50	5.1	0.45	1814	0.4	3.0	-11.2	77	2306	2614	0.48	0.54
75.3	2.4	725.1	2.2	800.4	2.7	0.49	6.4	0.57	1780	0.4	3.0	-12.2	76	2266	2569	0.47	0.54
100.3	2.4	700.1	2.2	800.4	2.3	0.43	7.3	0.66	1770	0.4	3.0	-12.7	75	2243	2542	0.47	0.53
125.2	2.5	675.6	2.2	800.8	2.3	0.44	7.2	0.65	1807	0.4	3.0	-12.8	75	2261	2563	0.46	0.53
150.0	2.5	650.1	2.2	800.1	2.3	0.44	7.9	0.72	1809	0.4	3.0	-13.0	75	2245	2546	0.46	0.52
200.0	2.7	600.0	2.3	800.0	2.9	0.55	7.4	0.67	1891	0.4	3.0	-12.6	76	2287	2592	0.45	0.51
**		800.2	3.4	800.2	3.0	0.81	3.3	0.37	2716	0.4	4.1	-9.2	110	2514	2762	0.50	0.55
0.2	0.1	800.1	3.4	800.3	3.1	0.81	3.3	0.36	2708	0.4	4.1	-4.3	111	2532	2782	0.51	0.56
5.0	1.8	795.0	3.6	800.0	2.3	0.61	3.5	0.38	2850	0.4	4.1	-8.6	112	2558	2810	0.49	0.54
10.1	3.0	790.3	3.5	800.4	2.4	0.61	3.6	0.38	2831	0.4	4.1	-8.7	112	2558	2810	0.50	0.55
15.0	3.5	786.0	3.7	801.0	2.0	0.51	3.4	0.35	2931	0.4	4.1	-8.3	114	2588	2843	0.49	0.54
25.0	3.6	774.4	3.6	799.4	1.9	0.45	4.4	0.45	2896	0.4	4.1	-8.6	113	2574	2828	0.49	0.54
50.1	3.6	750.4	3.5	800.5	2.0	0.48	5.2	0.51	2790	0.4	4.1	-9.5	113	2579	2834	0.51	0.56
75.1	3.8	725.3	3.5	800.4	2.2	0.50	4.7	0.45	2858	0.4	4.1	-9.2	116	2648	2908	0.53	0.58
100.2	3.8	700.3	3.5	800.5	2.6	0.58	4.5	0.43	2817	0.4	4.1	-9.4	116	2648	2908	0.54	0.59
125.3	3.9	675.3	3.5	800.6	2.7	0.58	4.5	0.42	2859	0.4	4.1	-9.3	117	2661	2923	0.53	0.59
150.1	4.0	650.9	3.5	801.0	2.8	0.58	4.5	0.42	2906	0.4	4.1	-9.1	117	2657	2919	0.52	0.57
175.3	4.1	624.9	3.5	800.2	3.2	0.66	5.3	4.85	2913	0.4	4.1	-9.4	115	2627	2885	0.51	0.57
200.6	4.1	600.4	3.4	801.0	3.6	0.72	6.6	0.60	2860	0.4	4.1	-11.0	114	2591	2846	0.50	0.56
**		801.1	4.4	801.0	2.3	0.81	4.2	0.65	3529	0.4	4.9	-10.0	146	2779	3004	0.56	0.61
0.3	0.2	801.0	4.4	801.3	2.3	0.81	4.3	0.64	3505	0.4	4.9	-9.9	145	2761	2985	0.56	0.61
5.0	2.3	795.2	4.4	800.2	2.0	0.68	4.2	0.60	3522	0.4	4.9	-9.9	145	2760	2984	0.56	0.60
10.1	4.0	790.6	4.4	800.7	2.4	0.78	3.2	0.43	3514	0.4	4.9	-9.2	143	2728	2949	0.54	0.59
15.1	4.4	786.0	4.4	801.1	2.4	0.78	4.0	0.52	3497	0.4	4.9	-9.3	142	2719	2939	0.54	0.59
25.3	4.5	775.6	4.4	800.9	2.4	0.72	3.9	0.48	3507	0.4	4.9	-9.3	143	2726	2947	0.54	0.59
50.2	4.6	750.5	4.3	800.7	2.1	0.63	5.1	0.60	3494	0.4	4.9	-9.9	143	2726	2947	0.55	0.59
75.0	4.8	725.6	4.3	800.6	2.4	0.67	5.6	0.64	3511	0.4	4.9	-10.2	143	2739	2960	0.55	0.59
100.7	4.9	700.0	4.3	800.7	2.8	0.75	6.9	0.77	3538	0.4	4.9	-10.7	144	2756	2979	0.55	0.60
125.4	5.0	675.4	4.4	800.8	3.1	0.81	5.7	0.61	3575	0.4	4.9	-10.3	145	2775	2999	0.55	0.60
150.0	5.1	650.6	4.4	800.6	3.4	0.84	4.7	0.49	3604	0.4	4.9	-9.8	145	2775	2999	0.55	0.59
175.2	5.2	625.6	4.4	800.8	3.8	0.91	5.6	0.57	3636	0.4	4.9	-10.1	146	2781	3006	0.55	0.59
200.1	5.3	600.2	4.4	800.3	3.6	0.82	5.7	0.57	3684	0.4	4.9	-10.2	146	2789	3014	0.54	0.59
**		800.8	5.4	800.8	5.5	1.12	7.3	0.77	4360	0.4	5.9	-8.9	185	2995	3197	0.62	0.67
5.1	3.1	795.2	5.6	800.3	4.2	0.86	6.7	0.69	4461	0.4	5.9	-9.6	183	2958	3158	0.60	0.64
10.2	5.4	790.5	5.6	800.7	3.5	0.71	5.5	0.56	4496	0.4	5.9	-9.4	183	2949	3149	0.59	0.63
25.4	5.8	775.7	5.5	801.1	3.4	0.68	6.7	0.66	4421	0.4	5.9	-9.9	180	2911	3108	0.58	0.62
50.3	6.0	750.6	5.5	800.9	3.8	0.75	6.6	0.64	4407	0.4	5.9	-10.0	181	2923	3121	0.59	0.63
75.2	6.2	725.1	5.5	800.3	3.9	0.75	7.2	0.70	4444	0.4	5.9	-10.1	181	2930	3128	0.59	0.63
100.6	6.3	700.5	5.5	801.1	4.6	0.87	9.1	0.86	4462	0.4	5.9	-10.8	183	2964	3165	0.60	0.64
125.3	6.3	675.1	5.5	800.4	4.8	0.91	6.8	0.63	4509	0.4	5.9	-10.0	184	2975	3176	0.60	0.64
150	6.42	650	5.5	800.0	4.9	0.89	7.5	0.682	4547	0.4	5.9	-10.1	185	2981	3182	0.59	0.63
175.3	6.55	624.6	5.52	799.9	5.0	0.889	7.6	0.681	4606	0.4	5.9	-10.1	184	2978	3180	0.58	0.63
200.1	6.61	599.1	5.52	799.2	4.7	0.821	8.9	0.779	4640	0.4	5.9	-10.4	184	2968	3169	0.58	0.62
**		800.4	6.5	800.4	5.2	1.30	8.6	0.91	5185	0.4	6.9	-10.3	224	3137	3320	0.67	0.71
0.5	0.3	800.3	6.5	800.8	5.0	1.19	8.8	0.90	5216	0.4	6.9	-10.4	224	3133	3315	0.66	0.70
2.2	1.0	799.1	6.6	801.3	7.5	1.21	8.1	0.67	5299	0.4	6.9	-9.0	224	3133	3316	0.65	0.69
2.9	2.0	796.8	6.7	799.7	6.6	1.04	8.8	0.71	5357	0.4	6.9	-9.0	226	3158	3342	0.65	0.69
4.3	3.2	796.8	6.7	801.1	6.3	0.99	9.0	0.72	5397	0.4	6.9	-8.8	226	3157	3341	0.65	0.69
5.6	4.0	794.1	6.8	799.7	6.5	0.99	8.4	0.67	5410	0.4	6.9	-8.6	225	3153	3337	0.64	0.68
7.5	5.3	793.0	6.8	800.5	6.7	0.86	8.6	0.67	5436	0.4	6.9	-8.7	225	3144	3327	0.64	0.68
9.9	5.9	790.7	6.8	800.6	6.0	0.89	8.8	0.68	5447	0.4	6.9	-8.6	225	3149	3332	0.64	0.68
16.0	7.0	784.8	6.8	800.8	5.9	0.86	8.9	0.68	5444	0.4	6.9	-8.7	225	3142	3325	0.64	0.67
25.0	7.3	775.4	6.7	800.4	6.0	0.87	9.2	0.71	5419	0.4	6.9	-8.8	224	3133	3315	0.64	0.67
50.0	7.5	750.4	6.7	800.4	5.4	0.91	9.3	0.70	5422	0.4	6.9	-8.8	223	3119	3301	0.63	0.67
75.1	7.7	725.3	6.7	800.4	6.5	0.91	8.9	0.67	5476	0.4	6.9	-8.8	224	3135	3318	0.63	0.67
100.2	7.8	700.1	6.8	800.3	6.5	0.90	11.1	0.84	5530	0.4	6.9	-9.2	225	3150	3333	0.63	0.67
125.1	7.9	675.0	6.8	800.1	6.6	0.90	10.7	0.80	5582	0.4	6.9	-9.2	226	3162	3346	0.63	0.67
150.2	8.0	650.5	6.8	800.7	6.1	0.82	10.9	0.81	5620	0.4	6.9	-9.3	225	3150	3334	0.62	0.66
175.1	8.0	625.3	6.7	800.4	6.6	0.89	13.4	1.00	5619	0.4	6.9	-9.9	225	3154	3338	0.62	0.66
200.5	8.1	600.4	6.8	800.9	7.0	0.92	11.7	0.86	5715	0.4	6.9	-9.4	226	3168	3353	0.62	0.65

*Indicates values calculated with discharge power only and without cathode flow.

**Indicates single stage point taken with anode electrodes electrically connected.



Figure 1: Laboratory model D-80 Hall thruster.



Legend:

1. First Stage anode
2. Second Stage Anode
3. Inner coil with magnetic pole
4. Outer coils (4) connected in series
5. Outer pole pieces
6. Flange
7. Guard rings
8. Insulators
9. Screen

Figure 2: Mechanical Schematic Drawing of D-80 Hall thruster.

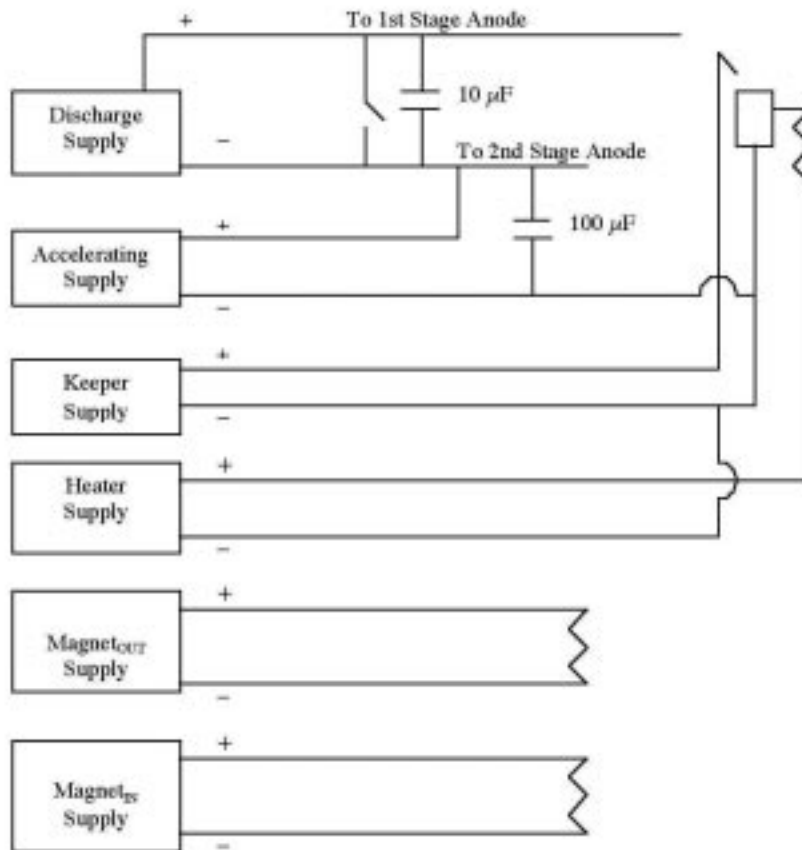


Figure 3: Electrical schematic drawing.



Figure 4: D-80 Hall thruster and test apparatus in NASA's Vacuum Facility 6.

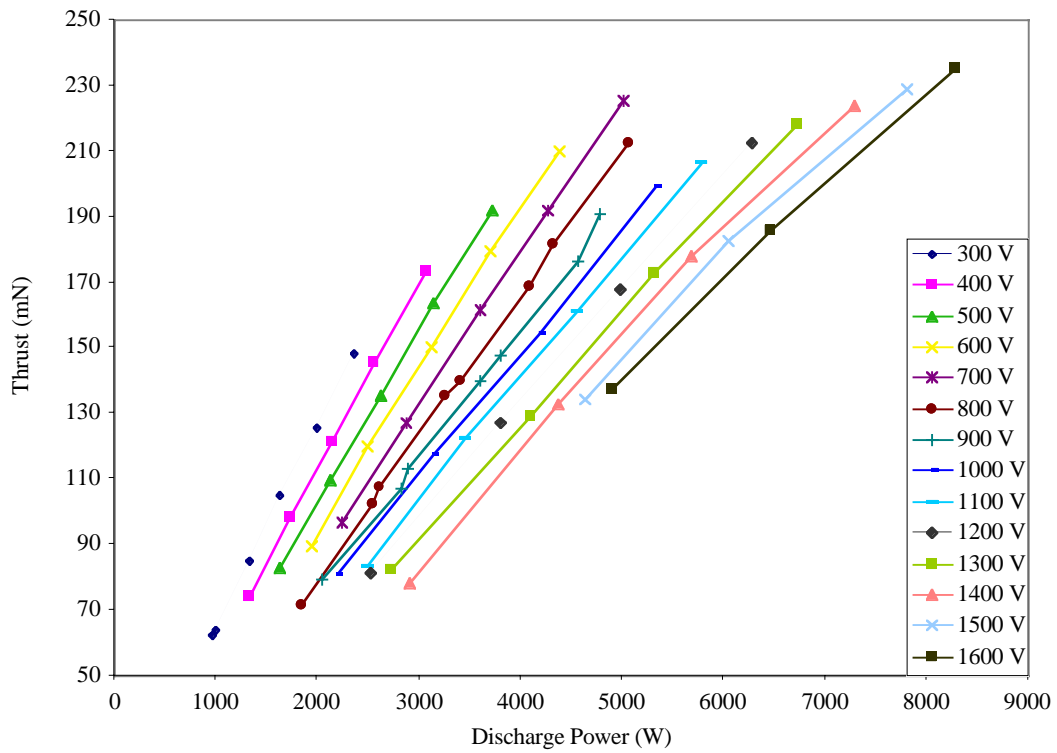


Figure 5: Single stage thrust versus discharge power.

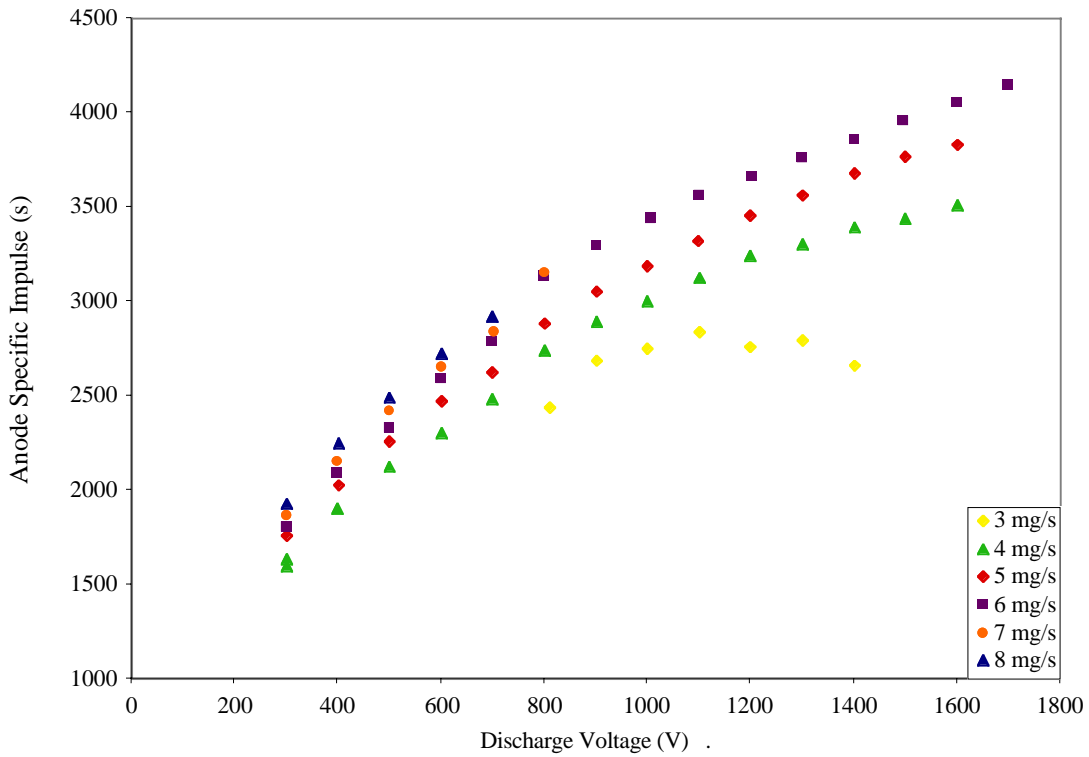


Figure 6: Single stage specific impulse versus discharge voltage.

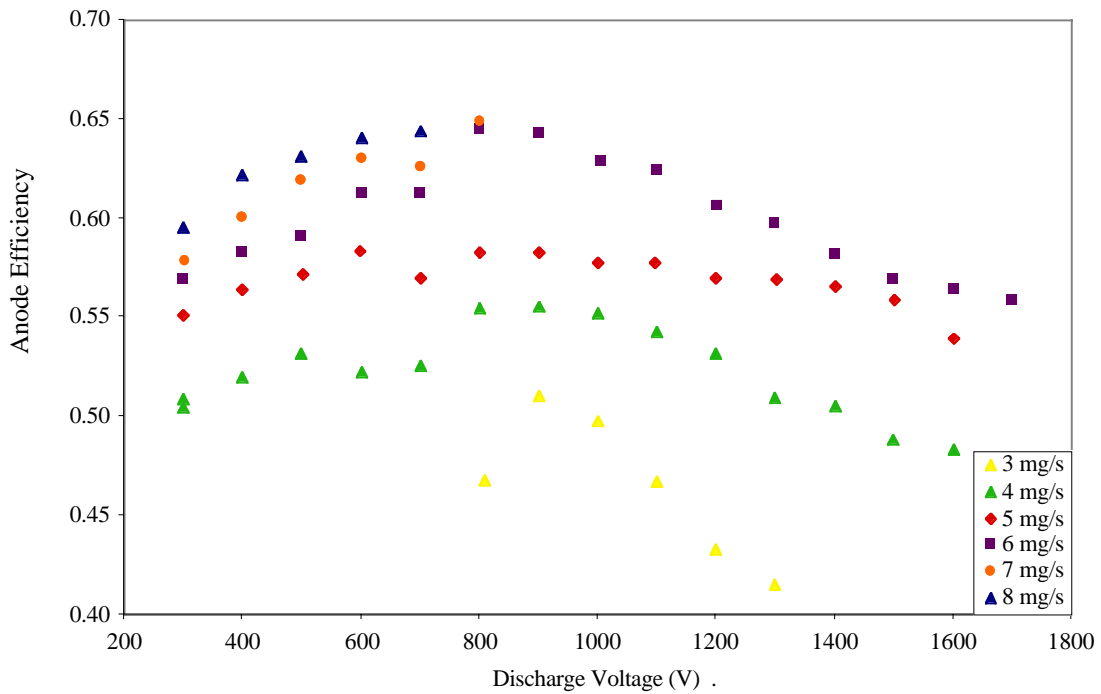


Figure 7: Single stage efficiency versus discharge voltage.

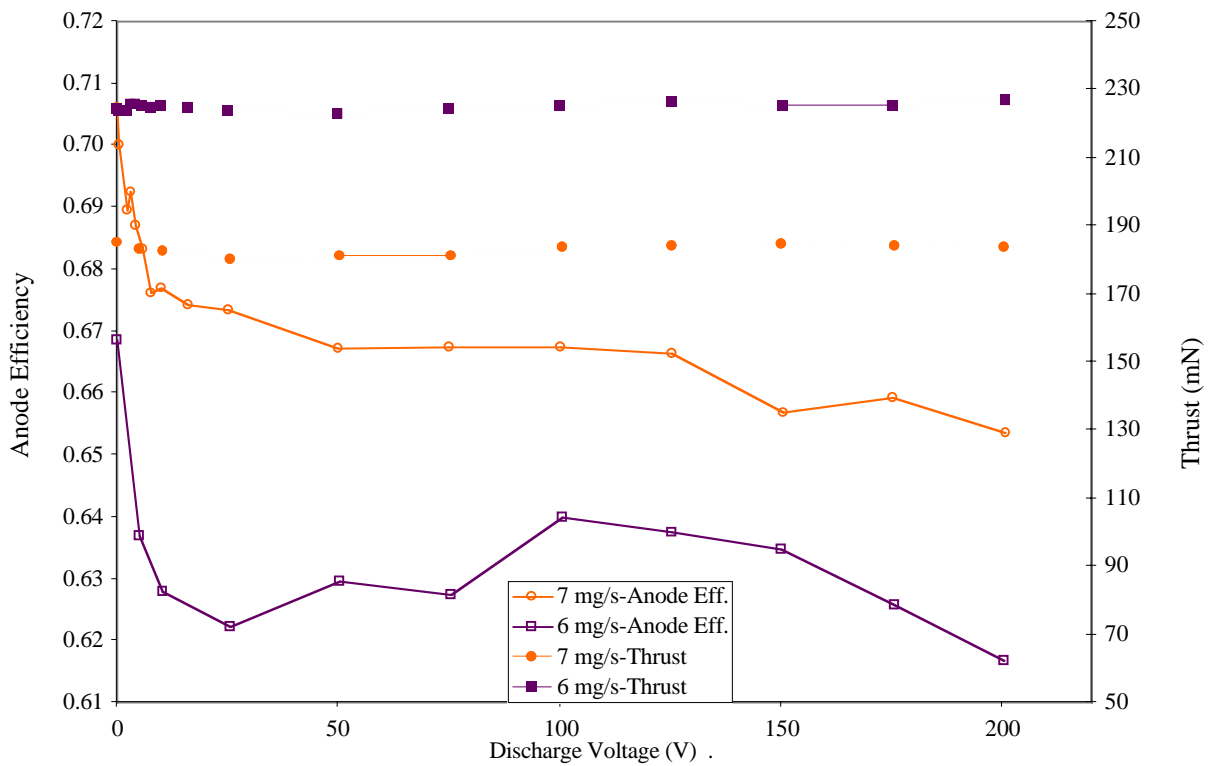


Figure 8: Two-stage anode efficiency and thrust versus discharge voltage for constant total voltage of 800 V

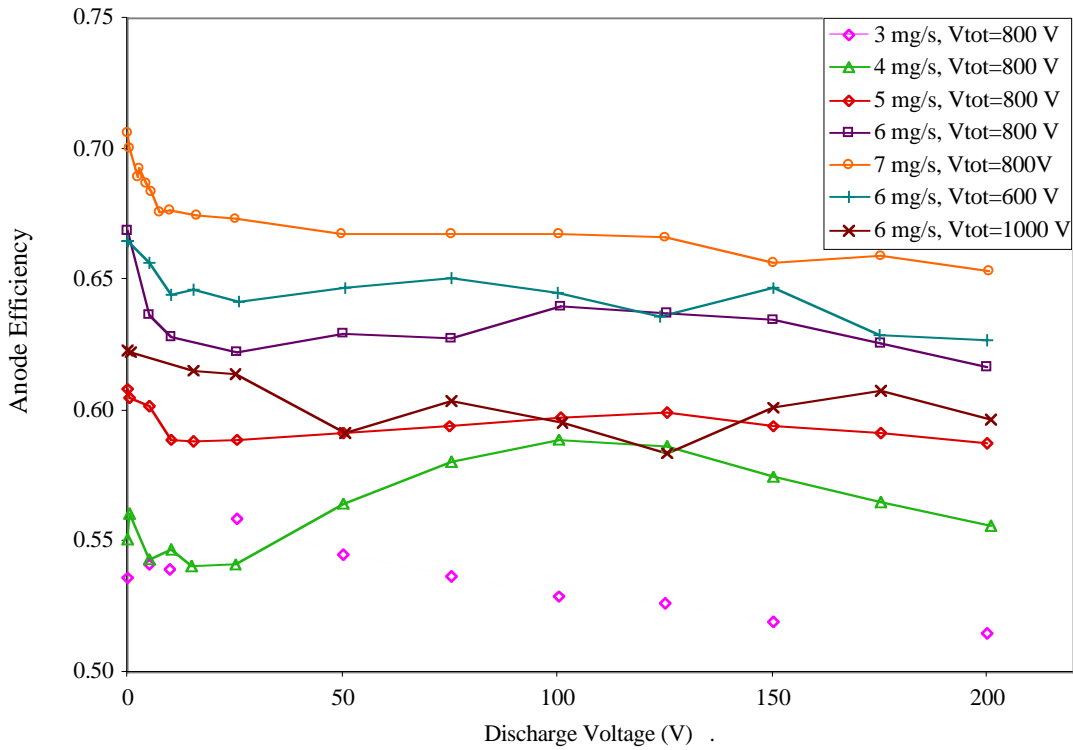


Figure 9: Two stage anode efficiency versus discharge voltage for total constant voltage cases.

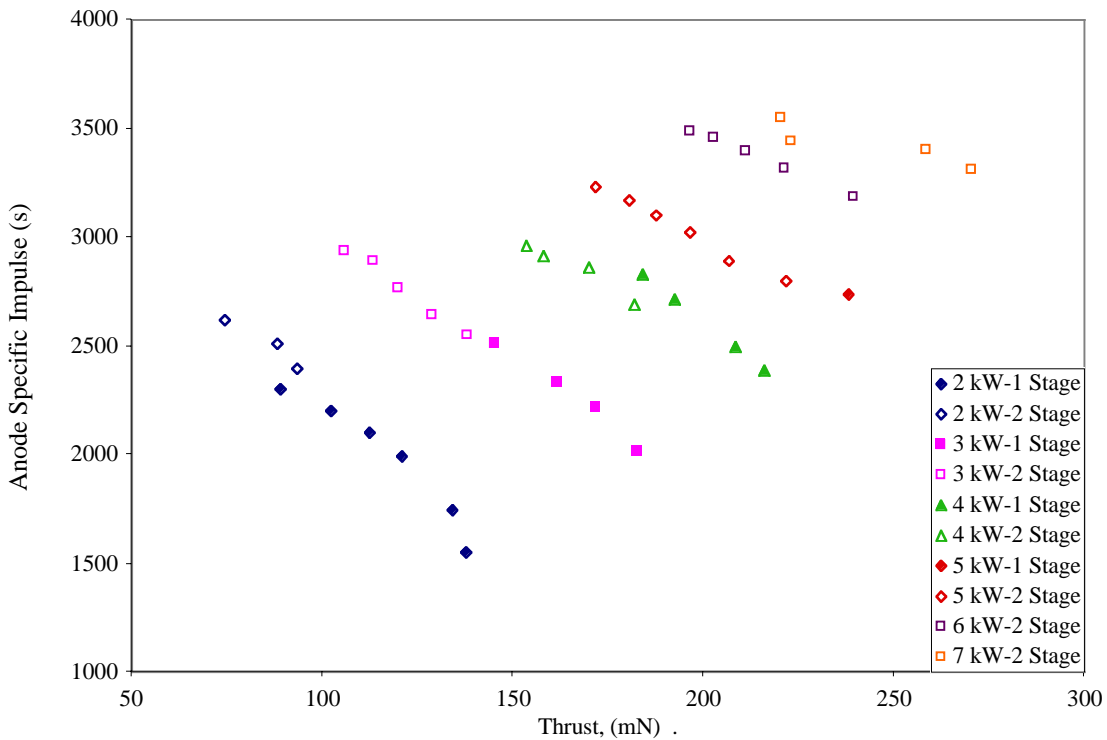


Figure 10: Single and two-stage specific impulse versus thrust for 2-7 kW power levels.

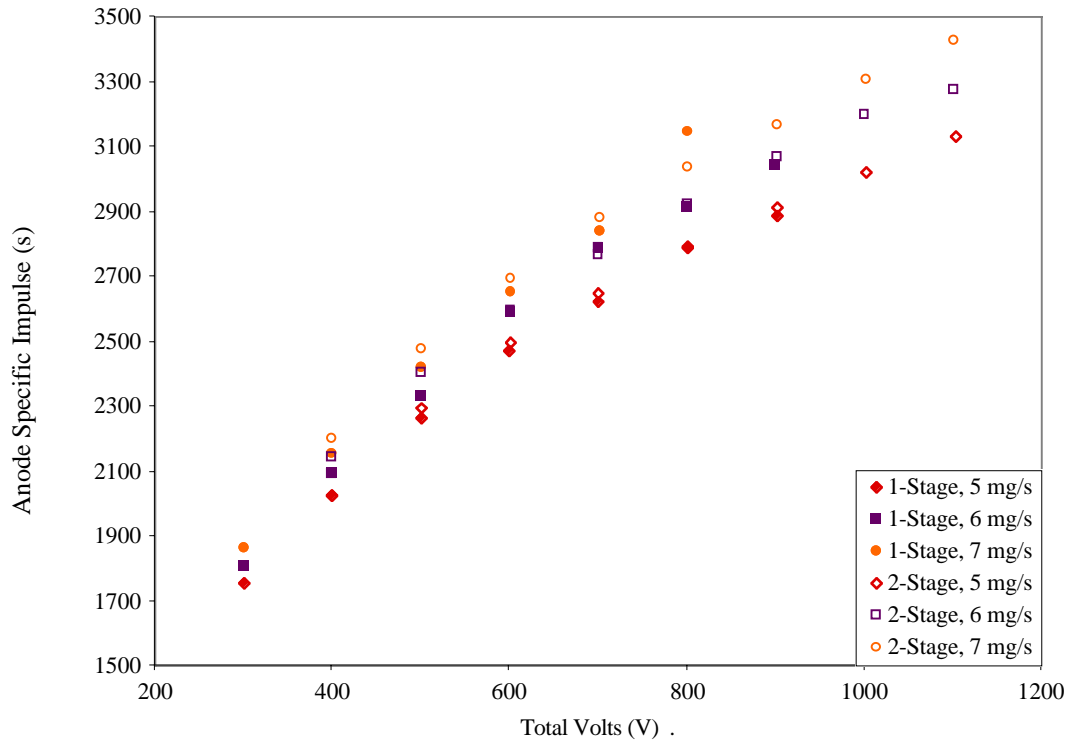


Figure 11: Comparison of single and two stage anode specific impulse for flow rates 5-7 mg/s.

REPORT DOCUMENTATION PAGE

Form Approved
OMB No. 0704-0188

Public reporting burden for this collection of information is estimated to average 1 hour per response, including the time for reviewing instructions, searching existing data sources, gathering and maintaining the data needed, and completing and reviewing the collection of information. Send comments regarding this burden estimate or any other aspect of this collection of information, including suggestions for reducing this burden, to Washington Headquarters Services, Directorate for Information Operations and Reports, 1215 Jefferson Davis Highway, Suite 1204, Arlington, VA 22202-4302, and to the Office of Management and Budget, Paperwork Reduction Project (0704-0188), Washington, DC 20503.

1. AGENCY USE ONLY (<i>Leave blank</i>)		2. REPORT DATE November 2001	3. REPORT TYPE AND DATES COVERED Technical Memorandum	
4. TITLE AND SUBTITLE High Voltage TAL Performance			5. FUNDING NUMBERS WU-755-B4-05-00	
6. AUTHOR(S) David T. Jacobson, Robert S. Jankovsky, Vincent K. Rawlin, and David H. Manzella				
7. PERFORMING ORGANIZATION NAME(S) AND ADDRESS(ES) National Aeronautics and Space Administration John H. Glenn Research Center at Lewis Field Cleveland, Ohio 44135-3191			8. PERFORMING ORGANIZATION REPORT NUMBER E-12999	
9. SPONSORING/MONITORING AGENCY NAME(S) AND ADDRESS(ES) National Aeronautics and Space Administration Washington, DC 20546-0001			10. SPONSORING/MONITORING AGENCY REPORT NUMBER NASA TM-2001-211147 AIAA-2001-3777	
11. SUPPLEMENTARY NOTES Prepared for the 37th Joint Propulsion Conference and Exhibit cosponsored by the AIAA, SAE, AIChE, and ASME, Salt Lake City, Utah, July 8-11, 2001. David T. Jacobson, Robert S. Jankovsky, and Vincent K. Rawlin, NASA Glenn Research Center; and David H. Manzella, University of Toledo, 2801 W. Bancroft Street, Toledo, Ohio 43606-3328. Responsible person, David T. Jacobson, organization code 5430, 216-433-3691.				
12a. DISTRIBUTION/AVAILABILITY STATEMENT Unclassified - Unlimited Subject Category: 20 Available electronically at http://gltrs.grc.nasa.gov/GLTRS This publication is available from the NASA Center for AeroSpace Information, 301-621-0390.			12b. DISTRIBUTION CODE	
13. ABSTRACT (<i>Maximum 200 words</i>) The performance of a two-stage, anode layer Hall thruster was evaluated. Experiments were conducted in single and two-stage configurations. In single-stage configuration, the thruster was operated with discharge voltages ranging from 300 to 1700 V. Discharge specific impulses ranged from 1630 to 4140 sec. Thruster investigations were conducted with input power ranging from 1 to 8.7 kW, corresponding to power throttling of nearly 9:1. An extensive two-stage performance map was generated. Data taken with total voltage (sum of discharge and accelerating voltage) constant revealed a decrease in thruster efficiency as the discharge voltage was increased. Anode specific impulse values were comparable in the single and two-stage configurations showing no strong advantage for two-stage operation.				
14. SUBJECT TERMS Hall thruster			15. NUMBER OF PAGES 21	
			16. PRICE CODE	
17. SECURITY CLASSIFICATION OF REPORT Unclassified	18. SECURITY CLASSIFICATION OF THIS PAGE Unclassified	19. SECURITY CLASSIFICATION OF ABSTRACT Unclassified	20. LIMITATION OF ABSTRACT	